Paper accepted for presentation at 2009 IEEE Bucharest Power Tech Conference, June 28th - July 2nd, Bucharest, Romania

A New DC Feeder Protection Based On Wavelet Transform

L Yu [1], J H He[1], Z Q Bo[2], M X Li [1], T Yip[2], A Klimek[2]

[1] Beijing Jiaotong University, China [2] AREVA T&D Automation, UK

***Abstract*--This paper presents a new DC feeder protection based on wavelet transform. The model of two substation rectifiers in one track section has been proposed which is according to practical situation. The remote short-circuit current is determined mainly by the steel rail impedance, which is time varying due to the skin effect. In contrast, impedances of the traction motor and the contact wires, and the change of operating mode during starting govern the train starting current. The wavelet transform identifies these salient features. The remote short-circuit current and train starting current are simulated using SIMULlNK. The modeling was conducted with respect to the variations of the starting-up process and short circuit conditions. By comparing and investigating the simulation results of short circuit current and the train starting current, more effective algorithms such as wavelet transform has been proposed.**

I. Introduction

The DC traction system of Beijing Metros is operating at 750V DC obtained from 10kV AC distribution station. In Shanghai and Shenzhen, the voltage is 1500V DC obtained from 35kV AC. Power supply is one of the important systems providing power to not only the trains but also other sub-systems and services such as signaling, lighting, ventilation, fire protection, etc. A typical DC traction power supply system is shown in Fig.1:

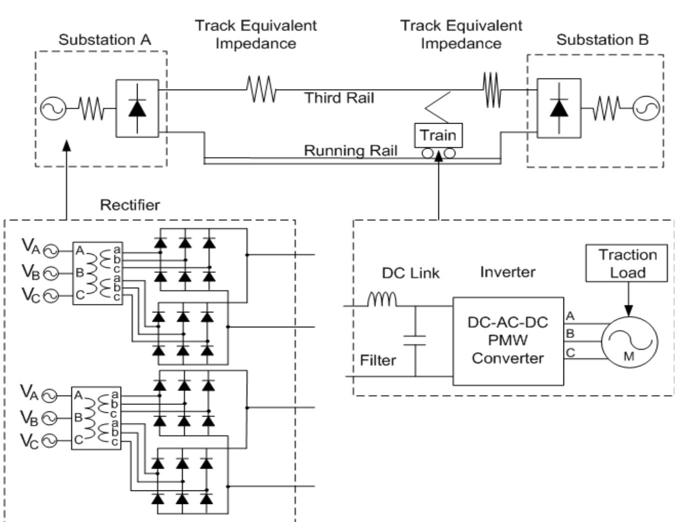

Fig. 1. Model of DC transit system

Le Yu is with school of electrical engineering in Beijing Jiaotong University, Beijing, China (e-mail: 0711733@bjtu.edu.cn).

In DC railways, the usual assumption of high remote short-circuit currents becomes insufficient, as high traffic density results in heavy train loads. Subsequent studies indicated that the former can have a lower initial rate of change *(di/dt)* and a longer duration than the typical train starting time. However, some researches [5] show that the methods are incapable of providing sufficiently consistent discrimination between the train starting current and remote short-circuit.

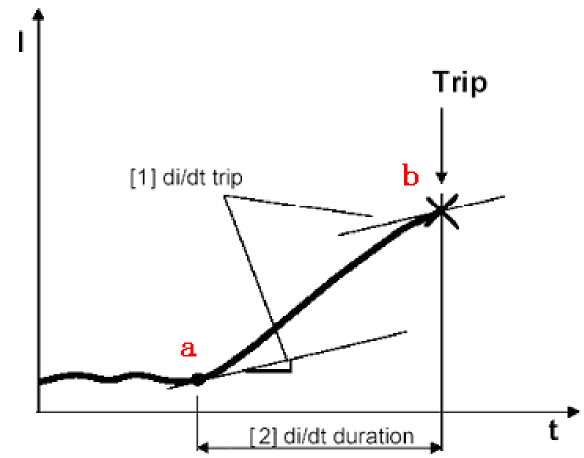

Fig. 2. Principle of di/dt- Δt protection di/dt- Δt

Point a--- Changing rate of current higher than trip setting level. [Start-up]

Point b--- The changing rate of current between a and b continuously higher than di/dt trip setting level and the duration not less than the setting level. [Trip]

Presently the current relays used in the detection of short-circuit faults in DC transit systems are based on current magnitude and gradient methods [2, 3]. These relays do not provide reliable detection of remote short circuit faults from the substation especially those of the DC-link fault type that occur within the train units. This is attributed to the similarity of the rise profile of the short circuit current and that of the starting current waveforms.

A wavelet-based signal processing technique is an effective tool for power system transient analysis and feature extraction. The method of wavelet transform is developed for capturing the different dynamic characteristics of the two currents. It is shown to be more effective and reliable than the di/dt comparison methods.

978-1-4244-2235-7/09/$25.00 ©2009 IEEE

II. Simulation Models

Fig.3 shows the train starting from a nearby substation.

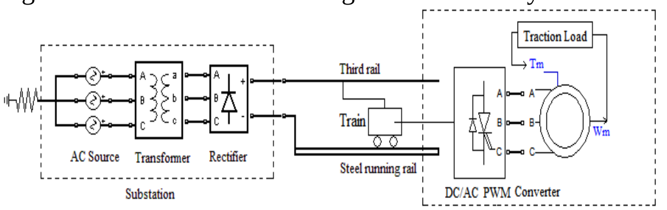

Fig. 3. Model of train starting

Fig.4 shows a remote short circuit fault occurring between the third rail and return running rails, with no moving train between the substation and fault.

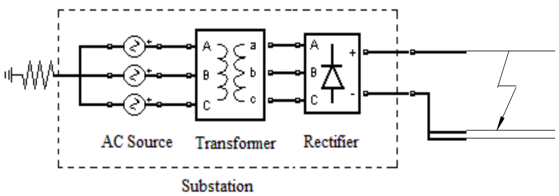

Fig. 4. Model of remote short-circuit

The timely detection of a DC short-circuit fault condition from a normal starting condition has been a common problem in DC transit systems. One such fault is the DC-link fault that takes place within the train. Fig. 4 illustrates the electrical diagram of a typical DC transit system [l]. The arrow in bold print indicates the location of the short-circuit fault that occurs across the DC-link capacitor, within the train electrical compartment.

A. SIMULINK models for remote short circuit

Because of the skin effects in the steel running rails, The model in Fig. 4 is implemented for the remote short-circuit track impedance, which comprises resistance, internal inductance and external inductance .

The substation with a three-phase rectifier is represented by an equivalent DC voltage source (1500V). The model ignores the tracking line shunt parameters, earth leakage and return path.

The complete SIMULINK model of whole DC transit system which consists of substation, traction load and locomotive subsystem is proposed in Fig. 5.

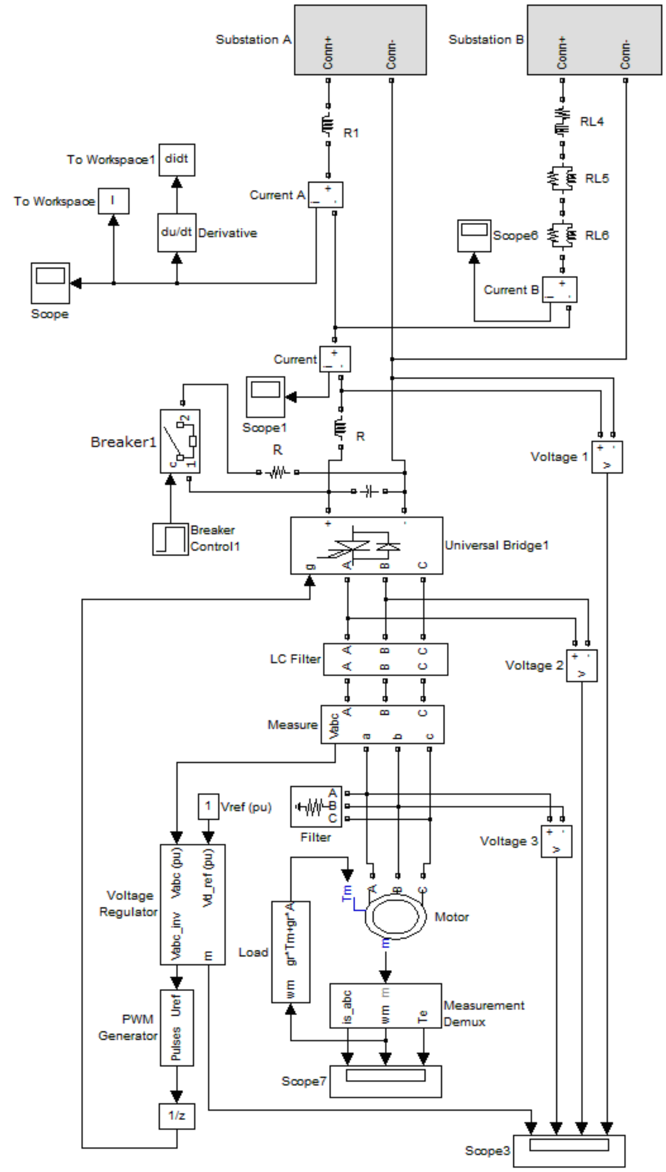

Fig. 5. SIMULINK model of DC transit system

B. Results of simulations

The study period in the SIMULINK simulations is 20 ms.

1) Train starting current

Using the SIMULINK model, which includes the equivalent resistance and inductance according to the fault distance from the substation, the remote short-circuit currents are simulated at two fault locations. Results in Fig.4 exhibit a time-varying time constant for each fault location as revealed by several other researchers.

When the train is being started, feeder line currents at each substation are given in Fig. 6. The simulation is based on the following assumptions:

(i) The track section is based on bilateral power supply system.

(ii) The train is started from substation B to substation A.

(iii) The total length of this track section is assumed to be 2km.

As shown in Fig.6, both the current rising rate and current increment increase when the distance from the substation is decreased. The maximum starting current could be more than three times of the operation current.

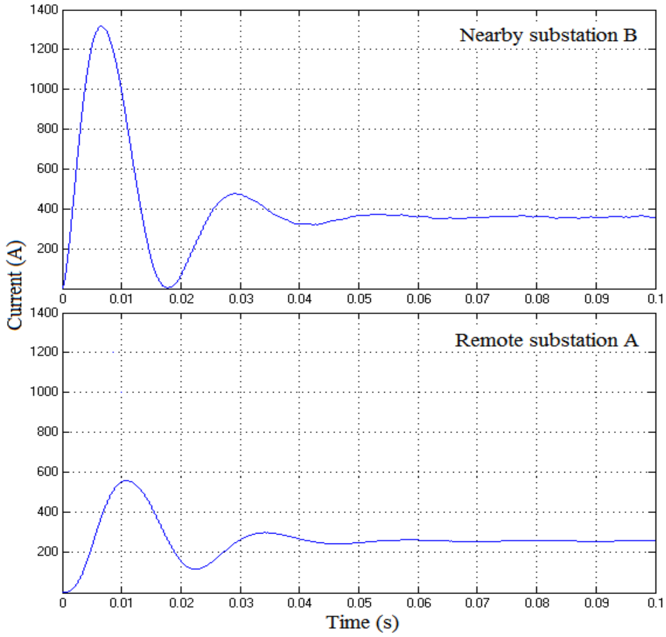

Fig. 6. Train starting current of different feeder lines at one track section

C. *Remote short-circuit current*

Actual remote short-circuit currents were recorded on the London Docklands Light Rail system [4]. The rising portion of each recording was divided into segments and curve-fitted for calculating the equivalent time constants using the following equation [4]:

$$i(t) = \frac{V}{R}[1 - \exp(-\frac{t}{\tau})] \qquad (1)$$

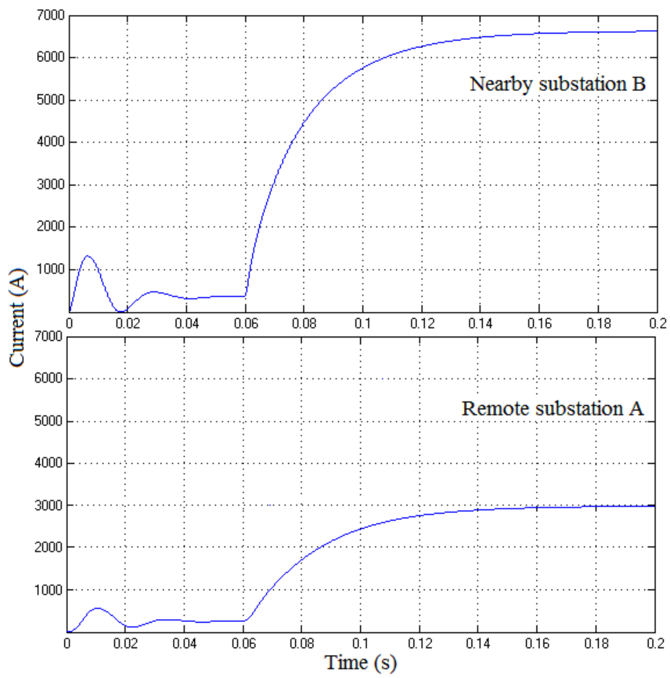

Fig. 7. Short circuit current of different feeder lines at one track section

III. Wavelet Transform

The feature-extraction process is introduced to enhance the difference in the DC surge profile between the normal starting and DC-link fault cases. The process takes place only after a surge is detected in the DC waveform. On detecting a surge, continuous wavelet transform (CWT) is performed on the current surge: data contained in the sliding window so as to extract the corresponding feature vector. The function of CWT is clearly different here as compared with when it is used in detecting the surge. The details of the feature extraction function of CWT are explained as follows.

The function by integrating it with scaled and translated versions of the kernel function $\psi(t)$. The kernel function is a zero-mean band-pass function with a short-duration cycle, known as a wavelet. The kernel function is similar to the sine or cosine function of the Fourier transform. It takes a variety of forms, but must satisfy the admissible condition in eqn. 4 in the time domain or eqn. *5* in the frequency domain, which means that the kernel function must quickly decay to zero during oscillations. The kernel function has the localisation property that works like a window in the time domain and like a band-pass filter in the frequency domain [6].

$$\int_{-\infty}^{\infty} \psi(t)dt = 0 \qquad (2)$$

$$\int_{-\infty}^{\infty} \frac{|\Psi(\omega)|^2}{|\omega|} d\omega < \infty \qquad (3)$$

The modified versions of the kernel function $\psi_{(a,b)}(t)$,'wavelets', are derived from $\psi(t)$ as:

$$\psi_{(a,b)}(t) = 1/\sqrt{a} * \psi(\frac{t-b}{a}) \qquad (4)$$

Eqn. 6 indicates that $\psi_{(a,b)}(t)$ is *a* scaled and translated version of the kernel function $\psi(t)$, and the normalization factor $(1/\sqrt{a})$ensures $\psi_{(a,b)}(t)$, as the same energy *as* the kernel function $\psi(t)$. In the wavelet transform, this kernel function $\psi(t)$ is known as the 'mother wavelet'. Scaling ***a*** mother wavelet simply means stretching (or compressing) it, and translating it means shifting it in the time domain. In eqn. 6, *a* represents the scaling factor and *b* represents the time translation parameter. When the scaling factor ***a*** > 1 ***(or a*** < 1), the mother wavelet is stretched (or compressed). The high scale value therefore corresponds to the low frequency, and the low scale value corresponds to the high frequency. Thus, for *a* given function *f(t),* its CWT is defined as:

$$W_\psi f(a,b) = |a|^{-\frac{1}{2}} \int f(x)\psi^*(\frac{t-b}{a})dx \qquad (5)$$

where (*) stands for the complex conjugate.

The Mexican-hat wavelet function is defined as

$$\psi(t) = (1-t^2)e^{-t^2/2} \qquad (6)$$

Thus, for a given function: $f(t) = \frac{V}{R}(1-e^{-\alpha t}) \ \ (0 < \alpha < 1)$,

its continuous Mexican-hat wavelet transform is:

$$W_\psi f(a,b) = \frac{V}{R} a^{-1/2} \int_{-\infty}^{\infty} (1-e^{-\alpha t})[1-(\frac{t-b}{a})]e^{-(\frac{t-b}{2})^2/2} dt \qquad (7)$$

Due to the integral of the mother wavelet equal to 0.

$$\int_{-\infty}^{\infty}[1-(\frac{t-b}{a})]e^{-(\frac{t-b}{2})^2/2}dt=0 \qquad (8)$$

Thus, the function of CWT can be expressed as：

$$W_{\psi}f(a,b)=-\frac{V}{R}a^{-1/2}\int_{-\infty}^{\infty}e^{-\alpha t}[1-(\frac{t-b}{a})]e^{-(\frac{t-b}{2})^2/2}dt \qquad (9)$$

Make $\frac{t-b}{a}=x$， so t= ax +b.

$$W_{\psi}f(a,b)=-\sqrt{a}\int_{-\infty}^{\infty}[e^{-\alpha(ax+b)}e^{-x^2/2}-x^2e^{-\alpha(ax+b)}e^{-x^2/2}]dx \qquad (10)$$

According to:

$$\int_{-\infty}^{\infty}e^{-\alpha(ax+b)}e^{-x^2/2}dx=\sqrt{2\pi}e^{(\alpha^2a^2/2-ab)} \qquad (11)$$

$$\int_{-\infty}^{\infty}t^2e^{-t^2/2}dt=\int_{-\infty}^{\infty}tde^{-t^2/2}=\sqrt{2\pi} \qquad (12)$$

$$\int_{-\infty}^{\infty}te^{-t^2/2}dt=0 \qquad (13)$$

The wavelet transform result is as follows:

$$W_{\psi}f(a,b)=\frac{V}{R}\sqrt{2a\pi}e^{\alpha^2a^2/2-ab}\alpha^2a^2 \qquad (14)$$

According to the result, the Mexican-hat transform can make the original wave shows the characteristic of exponential function.

1) Results of wavelet transform

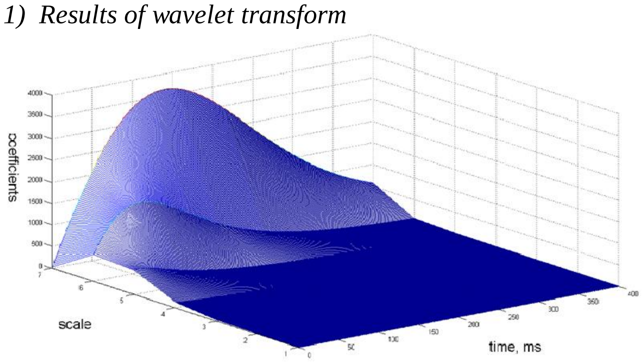

Fig. 8. CWT results of the remote short-circuit current using Mexican-hat transform

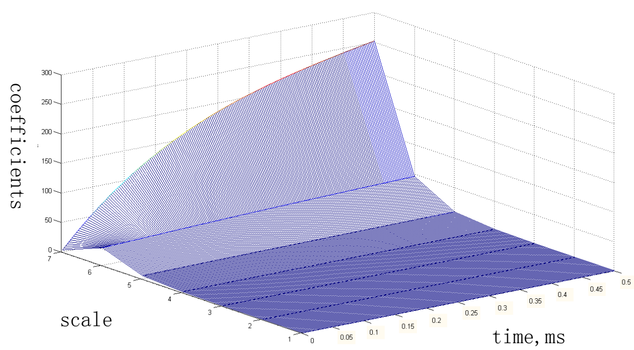

Fig. 9. CWT results of the train starting current using Mexican-hat transform

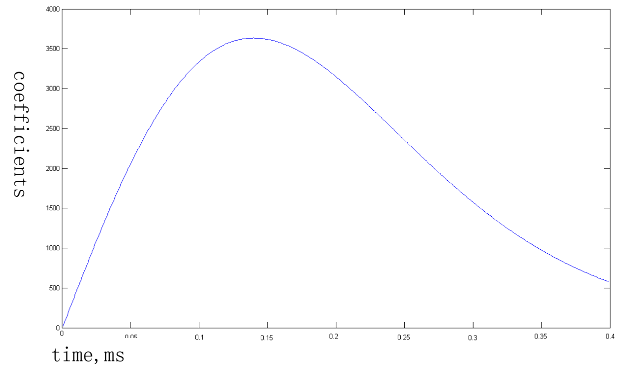

Fig. 10. CWT results of the remote short-circuit current using Mexican-hat transform (scale=7)

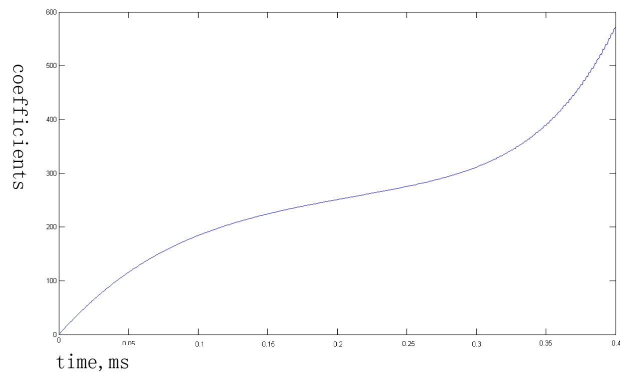

Fig. 11. CWT results of the train starting current using Mexican-hat transform (scale=7)

When scale= 7, the scaling factor a=128, the CWT results of the train starting current displayed in Fig. 11 exhibits an exponential function waveform. According to eqn.13, when α is constant, the waveform of eqn. exhibits like an exponential function, which is conformed with the result.

The CWT results of remote short-circuit current displayed in Fig.10 exhibits a waveform first increases then decreases. According to eqn.13, when α decreases, the waveform of fig.10 is conformed with the result.

According to the results of the wavelet transform starting current and short-circuit current, it is easy to find the difference between them.

IV. Wavelet Analysis for Discrimination

In the following analysis, the wavelet results are presented in 3-dimensional displays, in which the x-axis represents the time interval, the y-axis represents the scales, and the z-axis represents the abs of wavelet coefficients.

The CWT results of the remote short-circuit current at 10Km distance from station is displayed in Fig.10, where the wavelet coefficients produce a characteristic surface that exhibits a continuously varying time constant or the short-circuit current.

The CWT results of the train-starting modes are displayed in Figs. 11.

A. Comparison of discrimination methods

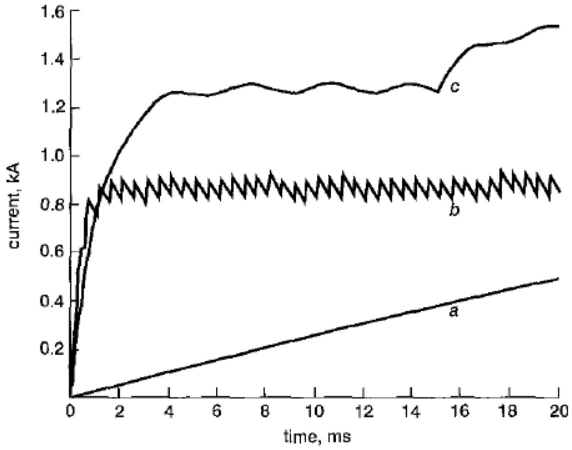

Fig. 12. Starting current profiles under different operation conditions
a: chopper has not taken effect
b:chopper has taken effect
c:with rheostatic

The current magnitude and *di/dt* comparison methods obviously provide inferior discrimination. If the former method is applied to Fig. *12a,* the method will fail to distinguish it from the remote short-circuit current because of the high magnitude of the initial rising part of the curve. If the latter method is applied to Fig. *12a*, the method will fail to distinguish it from the remote short-circuit current because of the slow *di/dt* of the initial rising part of the curve [6].

Based on the above analysis, the wavelet transform is seen to offer a reliable detection of a remote fault by accurately discriminating it from the train starting current.

V. Conclusion

The SIMULINK model offers the waveforms of starting current and remote short-circuit current. The Mexican-hat wavelet transform can reveal the characteristics of the exponential function from these waveforms. Through the analysis of wavelet transform results, the properties of these two currents can be easily identified when scale=7.

VI. reference

Papers from Conference Proceedings (Published):

[1] R. Matthew, F. Flinders, W. Oghana, "Locomotive "Total System" Simulation Using Simulink", Electrical Railways in *United Europe, 27-30 March 1995, Conference Publication No.405, IEE 1995*

[2] Fracchia. M, Hill. R. J, Pozzobon. P, Sciutto. G, "Accurate track modelling for fault current studies on third-rail metro railways", *Railroad Conference, 1994., Proceedings of the 1994 ASME/IEEE Joint (in Conjunction with Area 1994 Annual Technical Conference), pp.97-102*

Periodicals:

[3] J.C. Brown, J. Allan, “Six-pulse three-phase rectifier bridge models for calculating close-up and remote short circuit transients on DC supplied railways”, *IEE Proc. B. Electr. Power Appl, 1991, 138, (6),, pp. 303-310,*
pp. 303-310

[4] J.C. Brown, J. Allan, B. Mellitt, “Calculation of remote short circuit fault currents for DC railways”, *IEE Proc. B. Electr. Power Appl, 1992, 139, (4),, pp. 289-294*

[5] CS. Chang, T. Feng, A. M. Khambadkone and S. Kumar, “Remote short circuit current determination in DC railway systems using wavelet transform”, *IEE Proc-Electr. Power Appl, Vol, 147, No. 6, November 2000, pp. 520-526*

[6] CS. Chang, A. Khambadkone, Zhao Xu, “Modeling and simulation of DCTransit system with VSI-fed Induction Motor Driven Train Using PSB/MATLAB”, *IEEE PEDS 2001 INDONESIA, pp. 881-885*

[7] Paolo Pozzobon, “Transient and Steady-State Short-Circuit Currents in Rectifiers for DC Traction Supply”, *IEEE Transactions on Vehicular Technology, VOL. 47, NO. 4, November 1998, pp. 1390-1404*

[8] Wei Kong, LiJun, Qin Q Yang, “Integrated Protection and Control, Network Management-Solution for DC Traction Power Supply System”, *IEE 2004*

[9] C.L. Pires, S.I. Nabeta, J.R. Cardoso, “Second-order model for remote and close-up short-circuit faults currents on DC traction supply”, *IET Power Electronics, 2008, Vol. 1, No. 3, pp. 348–355*

[10] Alberto Berizzi, Andrea Silvestri, Dario Zaninelli, Stefan0 Massucco, “Short-Circuit Current Calculations for DC Systems”, *IEEE Transactions on Industry Applications, vol. 32, no. 5, septembewoctober 1996, pp. 990-997*

VII. Biographies

Le Yu received his BSc in 2006 in the Department of Electrical engineering and Automation, Beijing Jiaotong University. Presently, he is working on his Ph.D. degree in the same field in Beijing Jiaotong University. His main research interests are Protective Relaying, Fault Distance Measurement and Location in Power System and Traction System.

Jinghan He received her BSc in 1987, MSc in 1994 in the Department of Automation, Tianjing University, China, respectively. Presently, She is employed as a Professor in Beijing JiaoTong University, China. Her main research interests are Protective Relaying, Fault distance measurement and Location in Power System.

Moxue Li received her BSc in 2007 in the Department of Electrical engineering and Automation, China Agriculture University. Presently, she is working on her MSc degree in the same field in Beijing Jiaotong University.

Her main research interests are Protective Relaying, Fault Distance Measurement and Location in Power System and Traction System.

Tony Yip received his M.Sc. in Digital Electronics and Ph.D. in Power System Protection, both from the University of Manchester in 1979 and 1988 respectively. He is a corporate member of the Institution of Engineering and Technology (I.E.T.) and a member of the CIGRE Working Group B5.04. He has been working in the Automation Product R&D Department in AREVA T&D Ltd in Stafford since 1979. His work is mainly related to the development of numerical protective relays. Currently he is a Product Development Team Leader, responsible for the development of generator, transformer and busbar protection relays.

Zhiqian Bo received his BSc degree from the Northeastern University, China in 1982 and PhD degree from The Queen's University of Belfast, UK in 1988 respectively. Presently, he is with AREVA T&D Automation & Information Business.

Andrew Klimek is a licensed Professional Engineer with B.Sc., M.Sc. degrees in Electrical Engineering. He has 34 years international experience in the electric power industry and is a member of CIGRE and IEEE. His experience includes a number of positions ranging from university teaching and consulting, to engineering and business management. Andrew has served as a project manager, marketing manager and general manager and has executed various power systems projects. Specifically, he has focused on power generation, transmission & distribution systems, SCADA, automation, protection and control. Cuffently Andrew is the technical Director of the AREVA T&D Automation & Information Business.